Inorg. Chem. **2008**, *47*, 6726−6737

Clarification of the Oxidation State of Cobalt Corroles in Heterogeneous and Homogeneous Catalytic Reduction of Dioxygen

Karl M. Kadish,*,† Jing Shen,† Laurent Frémond,† Ping Chen,† Maya El Ojaimi,‡ Mohammed Chkounda,‡ Claude P. Gros,‡ Jean-Michel Barbe,‡ Kei Ohkubo,§ Shunichi Fukuzumi,*,§ and Roger Guilard*,‡

Department of Chemistry, University of Houston, Houston, Texas 77204-5003, Université de Bourgogne, ICMUB (UMR 5260), 9, Avenue Alain Savary, BP 47870, 21078 Dijon Cedex France, and Department of Material and Life Science, Graduate School of Engineering, Osaka University, SORST, Japan Science and Technology Agency (JST), Suita, Osaka 565-0871, Japan

Received March 12, 2008

Co(III) corroles were investigated as efficient catalysts for the reduction of dioxygen in the presence of perchloric acid in both heterogeneous and homogeneous systems. The investigated compounds are (5,10,15-tris(pentafluorophenyl)corrole)cobalt (TPFCor)Co, (10-pentafluorophenyl-5,15-dimesitylcorrole)cobalt (F_5PhMes_2Cor)Co, and (5,10,15-trismesitylcorrole)cobalt (Mes_3Cor)Co, all of which contain bulky substituents at the three *meso* positions of the corrole macrocycle. Cyclic voltammetry and rotating ring-disk electrode voltammetry were used to examine the catalytic activity of the compounds when adsorbed on the surface of a graphite electrode in the presence of 1.0 M perchloric acid, and this data is compared to results for the homogeneous catalytic reduction of O_2 in benzonitrile containing 10^{-2} M $HClO_4$. The corroles were also investigated as to their redox properties in nonaqueous media. A reversible one-electron oxidation occurs at $E_{1/2}$ values between 0.42 and 0.89 V versus SCE depending upon the solvent and number of fluorine substituents on the compounds, and this is followed by a second reversible one-electron abstraction at $E_{1/2}$ = 0.86 to 1.18 V in CH_2Cl_2, THF, or PhCN. Two reductions of each corrole are also observed in the three solvents. A linear relationship is observed between $E_{1/2}$ for oxidation or reduction and the number of electron-withdrawing fluorine groups on the compounds, and the magnitude of the substituent effect is compared to what is observed in the case of tetraphenylporphyrins containing *meso*-substituted C_6F_5 substituents. The electrochemically generated forms of the corrole can exist with Co(I), Co(II), or Co(IV) central metal ions, and the site of the electron-transfer in each oxidation or reduction of the initial Co(III) complex was examined by UV−vis spectroelectrochemistry. ESR characterization was also used to characterize singly oxidized (F_5PhMes_2Cor)Co, which is unambiguously assigned as a Co(III) radical cation rather than the expected Co(IV) corrole with an unoxidized macrocyclic ring.

Introduction

Cobalt corroles are by far the most studied of any metallocorrole complexes.[1–20] The air-stable form of the compound contains Co(III) in the absence of axial ligands, but chloro-[21] and phenyl-[3] cobalt(IV) corroles have been structurally characterized. The oxidized and reduced forms of cobalt corroles can also be in situ generated and spectroscopically characterized in nonaqueous media.[1–7] The Co(III) and Co(II) forms of the corroles will strongly coordinate solvent molecules, nitrogenous bases, and anions,[2,21–26] whereas Co(III) corroles can axially bind a

* To whom correspondence should be addressed. E-mail: kkadish@uh.edu (K.M.K.), Roger.Guilard@u-bourgogne.fr (R.G.), fukuzumi@chem.eng.osaka-u.ac.jp (S.F.).
† University of Houston.
‡ Université de Bourgogne.
§ Osaka University.

(1) Erben, C.; Will, S.; Kadish, K. M. In *The Porphyrin Handbook*; Kadish, K. M., Smith, K. M., Guilard, R. Eds.; Academic Press: Boston, 2000; Vol. 2, pp 233−300.
(2) Guilard, R.; Barbe, J.-M.; Stern, C.; Kadish, K. M. In *The Porphyrin Handbook*; Kadish, K. M., Smith, K. M., Guilard, R. Eds.; Academic Press: Boston, 2003; Vol. 18, pp 303−349.
(3) Will, S.; Lex, J.; Vogel, E.; Adamian, V. A.; Van Caemelbecke, E.; Kadish, K. M. *Inorg. Chem.* **1996**, *35*, 5577–5583.

10.1021/ic800458s CCC: $40.75
Published on Web 06/27/2008

single CO molecule[22–24,27–30] or act as a catalyst for the electroreduction of O_2 in acid media.[21,31–33] Doubly reduced Co(III) corroles, which formally contain Co(I), have been spectroscopically characterized in acetonitrile. The Co(I) form of the corrole is stable in polar organic solvents but has been shown to catalytically reduce CO_2 in nonaqueous media.[20]

There have been extensive studies on the catalytic reduction of O_2 using cobalt porphyrins,[34–39] cobalt corroles,[31] and dyads containing one porphyrin and one cobalt corrole linked in a face-to-face arrangement.[21,31–33] The main difference between the cobalt corrole and cobalt porphyrin catalysts is the oxidation state of the central metal ion in the neutral compound. Uncharged cobalt porphyrins generally contain a Co(II) ion in their air stable form, whereas cobalt corroles contain Co(III) as a result of the −3 charge on the macrocycle. In the case of the Co(II) porphyrins, the oxidized species are well established to be Co(III) porphyrins rather than a radical cation of the porphyrin with the same metal oxidation state, that is, Co(II). In the case of Co(III) corroles, however, it has not been clearly established whether the oxidized species is in all cases a Co(IV) corrole as has been previously observed[4,5] or a radical cation of the corrole containing Co(III).

We clarify this point in the present study by examining the electrochemistry and spectroscopic properties of the three *meso*-substituted corroles shown in Chart 1. The compounds electrogenerated in each redox reaction can exist with Co(I), Co(II), Co(III), or Co(IV) central metal ions, and the site of each electron addition or abstraction was examined by UV−vis spectroelectrochemistry. These compounds differ from a previously examined compound, $(Me_4Ph_5Cor)Co$,[7,31] in that they contain bulky substituents at the three *meso*-positions of the macrocycle, which influence not only the half-wave potentials for oxidation and reduction but also diminish the ability of the corroles to dimerize in solution or at an electrode surface. The ability of **1**–**3** to act as homogeneous and heterogeneous catalysts in the reduction of O_2 is also investigated in acid media, and the singly oxidized cobalt corrole products are characterized by UV−vis and/or ESR spectroscopy.

Experimental Section

Chemicals and Compounds. Neutral alumina (Merck; usually Brockmann grade III, i.e. deactivated with 6% water) was used for column chromatography. Reactions were monitored by thin-layer chromatography and UV−vis spectroscopy. Pyridine (py, ≥99.8%), tetrahydrofuran (THF, ≥99.9%), and tetra-*n*-butylammonium chloride (TBACl, ≥99.5%) were obtained from Sigma-Aldrich Chemical Co. and used as received. Absolute dichloromethane (CH_2Cl_2) was obtained from EMD Chemical Inc. and used without further purification. Benzonitrile (PhCN) was purchased from Sigma-Aldrich Chemical Co. and distilled over P_2O_5 under reduced pressure prior to use. Tetra-*n*-butylammonium perchlorate (TBAP, Fluka Chemical Co.) was twice recrystallized from absolute ethanol and dried in a vacuum oven at 40 °C for 1 week prior to use. Perchloric acid ($HClO_4$, 70%) was purchased from Sigma-Aldrich Chemical Co. Aqueous solutions of 1 M $HClO_4$ were prepared with deionized water of resistivity not less than 18 MΩ cm. High-purity N_2 gas was purchased from Matheson-Trigas.

10-(pentafluorophenyl)-5,15-bis(2,4,6-trimethylphenyl)corrole, $(F_5PhMes_2Cor)H_3$, 5,10,15-tris(pentafluorophenyl)corrole (TPFCor)H_3,

(4) Adamian, V. A.; D'Souza, F.; Licoccia, S.; Di Vona, M. L.; Tassoni, E.; Paolesse, R.; Boschi, T.; Kadish, K. M. *Inorg. Chem.* **1995**, *34*, 532–540.
(5) Kadish, K. M.; Adamian, V. A.; Van Caemelbecke, E.; Gueletti, E.; Will, S.; Erben, C.; Vogel, E. *J. Am. Chem. Soc.* **1998**, *120*, 11986–11993.
(6) Kadish, K. M.; Koh, W.; Tagliatesta, P.; D'Souza, F.; Paolesse, R.; Licoccia, S.; Boschi, T. *Inorg. Chem.* **1992**, *31*, 2305–2313.
(7) Kadish, K. M.; Shao, J.; Ou, Z.; Gros, C. P.; Bolze, F.; Barbe, J.-M.; Guilard, R. *Inorg. Chem.* **2003**, *42*, 4062–4070.
(8) Johnson, A. W. *Pure Appl. Chem.* **1970**, *23*, 375–389.
(9) Hush, N. S.; Dyke, J. M. *J. Inorg. Nucl. Chem.* **1973**, *35*, 4341–4347.
(10) Hush, N. S.; Dyke, J. M.; Williams, M. L.; S., W. I. *J. Chem. Soc., Dalton Trans.* **1974**, 395–399.
(11) Hush, N. S.; Woolsey, I. S. *J. Chem. Soc., Dalton Trans.* **1974**, 24–34.
(12) Paolesse, R.; Licoccia, S.; Fanciullo, M.; Morgante, E.; Boschi, T. *Inorg. Chim. Acta* **1993**, *203*, 107–114.
(13) Paolesse, R.; Licoccia, S.; Bandoli, G.; Dolmella, A.; Boschi, T. *Inorg. Chem.* **1994**, *33*, 1171–1176.
(14) Licoccia, S.; Paolesse, R. *Struct. Bonding (Berlin)* **1995**, *84*, 71–133.
(15) Genokhova, N. S.; Melent'eva, T. A.; Berezovskii, V. M. *Russ. Chem. Rev. (Engl. Transl.)* **1980**, *49*, 2132–2158.
(16) Melent'eva, T. A. *Russ. Chem. Rev. (Engl. Transl.)* **1983**, *52*, 1136–1172.
(17) Murakami, Y.; Yamada, S.; Matsuda, Y.; Sakata, K. *Bull. Chem. Soc. Jpn.* **1978**, *51*, 123–129.
(18) Murakami, Y.; Matsuda, Y.; Sakata, K.; Yamada, S.; Tanaka, Y.; Aoyama, Y. *Bull. Chem. Soc. Jpn.* **1981**, *54*, 163–169.
(19) Conlon, M.; Johnson, A. W.; Overend, W. R.; Rajapaksa, D.; Elson, C. M. *J. Chem. Soc., Perkin Trans. I* **1973**, 2281–2288.
(20) Grodkowski, J.; Neta, P.; Fujita, E.; Mahammed, A.; Simkhovich, L.; Gross, Z. *J. Phys. Chem A* **2002**, *106*, 4772–4778.
(21) Kadish, K. M.; Shao, J.; Ou, Z.; Frémond, L.; Zhan, R.; Burdet, F.; Barbe, J.-M.; Gros, C. P.; Guilard, R. *Inorg. Chem.* **2005**, *44*, 6744–6754.
(22) Guilard, R.; Jérôme, F.; Barbe, J.-M.; Gros, C. P.; Ou, Z.; Shao, J.; Fischer, J.; Weiss, R.; Kadish, K. M. *Inorg. Chem.* **2001**, *40*, 4856–4865.
(23) Kadish, K. M.; Ou, Z.; Shao, J.; Gros, C. P.; Barbe, J.-M.; Jérôme, F.; Bolze, F.; Burdet, F.; Guilard, R. *Inorg. Chem.* **2002**, *41*, 3990–4005.
(24) Guilard, R.; Gros, C. P.; Bolze, F.; Jérôme, F.; Ou, Z.; Shao, J.; Fischer, J.; Weiss, R.; Kadish, K. M. *Inorg. Chem.* **2001**, *40*, 4845–4855.
(25) Guilard, R.; Burdet, F.; Barbe, J.-M.; Gros, C. P.; Espinosa, E.; Shao, J.; Ou, Z.; Zhan, R.; Kadish, K. M. *Inorg. Chem.* **2005**, *44*, 3972–3983.
(26) Kadish, K. M.; Shao, J.; Ou, Z.; Zhan, R.; Burdet, F.; Barbe, J.-M.; Gros, C. P.; Guilard, R. *Inorg. Chem.* **2005**, *44*, 9023–9038.
(27) Barbe, J.-M.; Burdet, F.; Espinosa, E.; Guilard, R. *Eur. J. Inorg. Chem.* **2005**, *6*, 1032–1041.
(28) Barbe, J.-M.; Canard, G.; Brandès, S.; Guilard, R. *Angew. Chem., Int. Ed.* **2005**, *44*, 3103–3106.
(29) Barbe, J.-M.; Canard, G.; Brandès, S.; Guilard, R. *Chem. Eur. J.* **2007**, *13*, 2118–2129.
(30) Barbe, J.-M.; Canard, G.; Brandès, S.; Jérôme, F.; Dubois, G.; Guilard, R. *Dalton Trans.* **2004**, 1208–1214.
(31) Kadish, K. M.; Frémond, L.; Ou, Z.; Shao, J.; Shi, C.; Anson, F. C.; Burdet, F.; Gros, C. P.; Barbe, J.-M.; Guilard, R. *J. Am. Chem. Soc.* **2005**, *127*, 5625–5631.
(32) Kadish, K. M.; Frémond, L.; Burdet, F.; Barbe, J.-M.; Gros, C. P.; Guilard, R. *J. Inorg. Biochem.* **2006**, *100*, 858–868.
(33) Guillard, R.; Jérôme, F.; Gros, C. P.; Barbe, J.-M.; Ou, Z.; Shao, J.; Kadish, K. M. *C. R. Acad. Sci. Series IIC: Chimie* **2001**, *4*, 245–254.
(34) Collman, J. P.; Denisevich, P.; Konai, Y.; Marrocco, M.; Koval, C.; Anson, F. C. *J. Am. Chem. Soc.* **1980**, *102*, 6027–6036.
(35) Collman, J. P.; Kaplun, M.; Decréau, R. A. *Dalton Trans.* **2006**, 554–559.
(36) Durand, R. R.; Bencosme, C. S.; Collman, J. P.; Anson, F. C. *J. Am. Chem. Soc.* **1983**, *105*, 2710–2718.
(37) Fukuzumi, S.; Mochizuki, S.; Tanaka, T. *Inorg. Chem.* **1989**, *28*, 2459–2465.
(38) Fukuzumi, S.; Okamoto, K.; Gros, C. P.; Guilard, R. *J. Am. Chem. Soc.* **2004**, *126*, 10441–10449.
(39) Fukuzumi, S.; Okamoto, K.; Tokuda, Y.; Gros, C. P.; Guilard, R. *J. Am. Chem. Soc.* **2004**, *126*, 17059–17066.

Chart 1. Investigated Monomeric Cobalt corroles

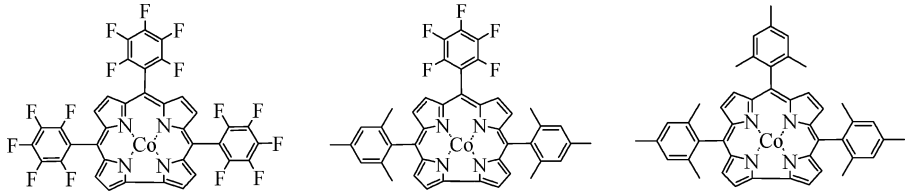

(TPFCor)Co (**1**) (F_5PhMes_2Cor)Co (**2**) (Mes_3Cor)Co (**3**)

and (5,10,15-tris(pentafluorophenyl)corrole)cobalt (TPFCor)Co (**1**) were synthesized according to literature procedures.[27,40–42] 5,10,15-trismesitylcorrole (Mes_3Cor)H_3 was synthesized according a method reported in ref 41 for *trans*-A_2B-corroles.

[10-Pentafluorophenyl-5,15-dimesitylcorrole]cobalt (F_5PhMes_2-Cor)Co (2). Under argon, a solution of 100 mg (0.143 mmol, 1 equiv) of the free-base corrole (F_5PhMes_2Cor)H_3, 52.5 mg (0.217 mmol, 1.5 equiv) of Co(II) acetate tetrahydrate in 10 mL of $CHCl_3$/methanol (70/30) was stirred and refluxed for 1 h 15 min, the metalation reaction being monitored by UV−vis spectroscopy and MALDI-TOF mass spectrometry. The solution was then poured into water (100 mL) and extracted with dichloromethane. The combined organic layers were dried over $MgSO_4$. After removal of the solvent in vacuo, the residue so obtained was redissolved in dichloromethane and chromatographed on alumina using CH_2Cl_2 as eluent. The title product **2** was isolated in 48% yield (52 mg, 0.069 mmol). MS (MALDI/TOF): m/z = 756.53 $[M]^{+\bullet}$; 756.17 Calcd for $C_{43}H_{30}F_5N_4Co$. UV−vis (CH_2Cl_2): λ_{max} ($\varepsilon \times 10^{-3}$ L mol^{-1} cm^{-1}) = 389.0 (59.8), 544.0 (7.6) nm. Anal. Calcd for $C_{43}H_{30}F_5N_4Co$: C, 68.26; H, 4.00; N, 7.40. Found: C, 67.97; H, 3.71; N, 7.06.

[5,10,15-trismesitylcorrole]cobalt (Mes_3Cor)Co (3). The trismesitylcorrole complex was synthesized as described above for **2**, starting from (Mes_3Cor)H_3 (170 mg, 0.261 mmol, 1 equiv) and 94.7 mg (0.392 mmol, 1.5 equiv) of Co(II) acetate tetrahydrate in 10% yield (18 mg, 0.025 mmol). MS (MALDI/TOF): m/z = 708.07 $[M]^{+\bullet}$; 708.27 Calcd for $C_{46}H_{41}N_4Co$. HR-MS (MALDI/TOF): 708.2613 $[M]^{+\bullet}$; 708.2657 Calcd for $C_{46}H_{41}N_4Co$. UV−vis (CH_2Cl_2): λ_{max} ($\varepsilon \times 10^{-3}$ L mol^{-1} cm^{-1}) = 390.1 (26.2) nm.

Instrumentation. Microanalyses were performed at the Université de Bourgogne on a Fisons EA 1108 CHNS instrument. Mass spectra and accurate mass measurements (HR-MS) were obtained on a Bruker Daltonics Ultraflex II spectrometer of the "Centre de Spectrométrie Moléculaire" in the MALDI/TOF reflectron mode using dithranol as a matrix. Cyclic voltammetry was carried out with an EG&G model 173 potentiostat/galvanostat. A three-electrode system was used and consisted of a glassy carbon or a platinum disk working electrode, a platinum wire counter electrode, and a saturated calomel reference electrode (SCE). The SCE electrode was separated from the bulk of the solution by a fritted-glass bridge of low porosity, which contained the solvent/supporting electrolyte. Half-wave potentials for reversible redox processes were determined by cyclic voltammetry and were calculated as $E_{1/2}$ = (E_{pa} + E_{pc})/2 where E_{pa} and E_{pc} represent the anodic and cathodic peak potentials, respectively. The $E_{1/2}$ values for irreversible redox processes in pyridine were obtained by the use of spectroelectrochemistry and the modified Nernst equation E_{app} = $E_{1/2}$ + (0.059/n)/log([ox]/[red]),[7,43] where [ox] represents the concentration of the Co(III) corrole in solution and [red] is the concentration of the singly reduced species. The latter value was determined from measurements of UV−vis spectra obtained during the electroreduction as previously described in the literature.[7]

Electrochemical measurements for the reduction of O_2 using the cobalt corroles as catalysts were carried out using a three-electrode system consisting of a platinum ring-graphite disk working electrode (Model MTI34, Pine Instruments Co.), a platinum wire as the auxiliary electrode, and an SCE reference electrode, which was separated from the bulk of the solution by means of a salt bridge. The rotating ring-disk electrode, purchased from the Pine Instrument Co., consisted of a platinum ring and a removable edge-plane pyrolytic graphite (EPPG) disk (A = 0.282 cm^2). Cyclic and rotating disk voltammograms were carried out using a Pine model AFMSR rotator linked to an EG&G Princeton Applied Research (PAR) model 263A potentiostat/galvanostat. The potentiostat was controlled by an IBM compatible PC microcomputer having an M270 (EG&G PARC) software package.

UV−vis spectroelectrochemical experiments were performed with an optically transparent platinum thin-layer electrode of the type described in the literature.[44] Potentials were applied with an EG&G PAR model 173 potentiostat. Time-resolved UV−vis spectra were recorded with a Hewlett-Packard Model 8453 diode array rapid-scanning spectrophotometer.

Homogeneous reduction of oxygen by 1,1′-dimethylferrocene $Fe(C_5H_4Me)_2$ in the presence of $HClO_4$ in PhCN was examined by monitoring the appearance of an absorption band due to the $[Fe(C_5H_4Me)_2]^+$ product (λ_{max} = 650 nm, ε_{max} = 290 M^{-1} cm^{-1})[38] using a Hewlett-Packard 8453 diode array spectrophotometer with a quartz cuvette (path length = 10 mm) at 298 K. An air-saturated PhCN solution was used for the catalytic reduction of oxygen by $Fe(C_5H_4Me)_2$. The O_2 concentration in an air-saturated PhCN solution (1.7×10^{-3} M) was determined as reported in the literature[38,45] and involved a spectroscopic titration for the photooxidation of 10-methyl-9,10-dihydroacridine by O_2. The concentrations of $Fe(C_5H_4Me)_2$ used for the catalytic reduction of O_2 were larger than the O_2 concentration in solution so that oxygen was the limiting reagent in the reaction cell, which was filled with the reactant solution.

Electrode Surface Preparation for O_2 Catalysis. Before use, the edge-plane pyrolytic graphite with the edges of the graphitic planes exposed was polished with 600 grit SiC paper, rinsed with purified water, and wiped off with clean tissue before it was coated with the catalytic film. The catalysts were adsorbed onto the graphite disk by transferring aliquots of a solution in $CHCl_3$ directly onto

(40) Gross, Z.; Golubkov, G.; Simkhovich, L. *Angew. Chem., Int. Ed.* **2000**, *39*, 4045–4047.
(41) Gryko, D. T.; Jadach, K. *J. Org. Chem.* **2001**, *66*, 4267–4275.
(42) Gros, C. P.; Brisach, F.; Meristoudi, A.; Espinosa, E.; Guilard, R.; Harvey, P. D. *Inorg. Chem.* **2007**, *46*, 125–135.
(43) Rohrbach, D. F.; Deutsch, E.; Heineman, W. R.; Pasternack, R. F. *Inorg. Chem.* **1977**, *16*, 2650–2652.
(44) Lin, X. Q.; Kadish, K. M. *Anal. Chem.* **1985**, *57*, 1498–1501.
(45) Fukuzumi, S.; Ishikawa, M.; Tanaka, T. *J. Chem. Soc., Perkin Trans. I* **1989**, 1037–1045.

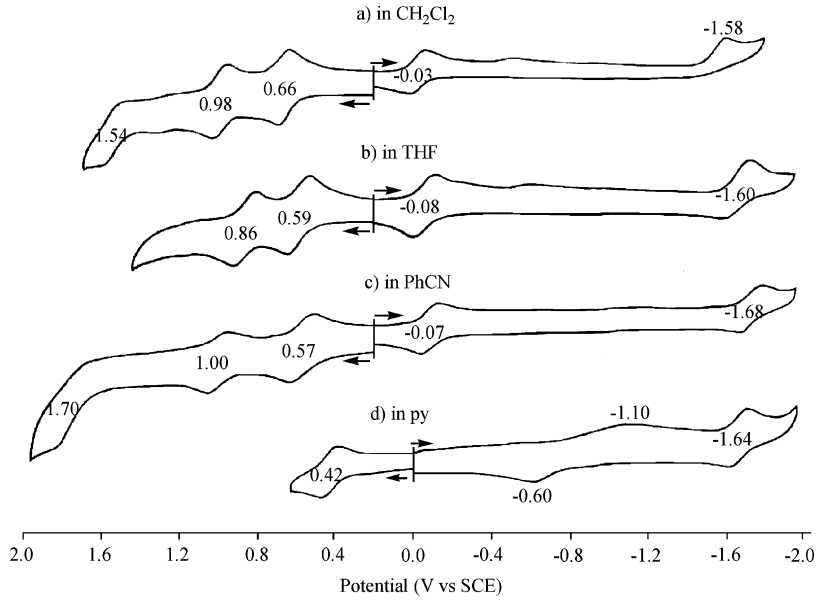

Figure 1. Cyclic voltammograms of (F_5PhMes_2Cor)Co (**2**) in (a) CH_2Cl_2, (b) THF, (c) PhCN, and (d) pyridine containing 0.1 M TBAP.

the electrode surface followed by evaporation of the solvent. Potentials were measured with respect to a saturated calomel reference electrode (SCE).

The slopes of the diagnostic Koutecky−Levich plots were determined by linear regression analysis of data acquired at 100, 300, 600, 900, 1600, 2500, and 3600 rpm (rotation per minute). The diffusion-limiting currents for the reduction of O_2 in aqueous solution at the rotating disk electrode were calculated using the following parameters: kinematic viscosity of H_2O at 25 °C, 0.01 $cm^2\ s^{-1}$; solubility of O_2 in air-saturated 1 M $HClO_4$, 0.24 mM; diffusion coefficient of O_2, $1.7 \times 10^{-5}\ cm^2\ s^{-1}$.[46]

ESR Measurements. ESR measurements were performed on a JEOL JES-FA100 ESR spectrometer and spectra were recorded under nonsaturating microwave power conditions. The magnitude of modulation was chosen to optimize the resolution and signal-to-noise (S/N) ratio of the observed spectra. The *g* values were calibrated with a Mn^{2+} marker.

Theoretical Calculations. Density-functional theory (DFT) calculations were performed on an 8CPU workstation (PQS, Quantum Cube QS8−2400C-064). Geometry optimizations were carried out using the Becke3LYP functional and 6−31G(d) basis set[47−50] with the restricted Hartree−Fock (RHF) formalism and as implemented in *Gaussian 03*, Revision C.02.[50] Graphical outputs of the computational results were generated with the *GaussView*, ver. 3.09, developed by Semichem, Inc.[51]

Table 1. Half-Wave Potentials (V vs SCE) of Co(III) Corroles in Different Solvents Containing 0.1 M TBAP

		ox			red	
solvent	compd				Co(III/II)	Co(II/I)
CH_2Cl_2	**1**		1.18	0.89	0.24	−1.37
	2	1.54	0.98	0.66	−0.03	−1.58[a]
	3	1.45	0.94	0.56	−0.18	[b]
PhCN	**1**		1.26	0.74	0.13	−1.40
	2	1.70	1.00	0.57	−0.07	−1.68
	3	1.64	0.87	0.48	−0.21	−1.74
THF	**2**		0.86	0.59	−0.08	−1.60
py	**2**			0.42	−0.77[c]	−1.64

[a] Peak potentials at a scan rate of 0.1 V/s. [b] Reaction not observed within cathodic potential window of solvent. [c] Reduction potential determined by monitoring changes in the spectra during electron addition and using the equation: $E_{app} = E_{1/2} + (0.059/n)\ \log([ox]/[red])$.

Results and Discussion

Electrochemistry in Nonaqueous Media. Each compound undergoes up to three oxidations and two reductions depending upon the solvent. Cyclic voltammograms illustrating the reduction and oxidation of **2** in four different nonaqueous solvents (CH_2Cl_2, THF, PhCN, and pyridine) containing 0.1 M TBAP are shown in Figure 1, and half-wave potentials for each redox reaction are summarized in Table 1, which also includes data for the other two investigated compounds. The electrochemical behavior of **1**−**3** in these solvents is similar to what has been earlier reported for other Co(III) corroles with different substituents,[1,2] namely each corrole undergoes a facile reduction to generate the Co(II) form of the compound, an additional one-electron reduction at negative potentials to generate the

(46) Shi, C.; Anson, F. C. *Inorg. Chem.* **1998**, *37*, 1037–1043.
(47) Becke, A. D. *J. Chem. Phys.* **1993**, *98*, 5648–5652.
(48) Hehre, W. J.; Radom, L.; Schleyer, P. v. R.; Pople, J. A. *Ab Initio Molecular Orbital Theory*; Wiley: New York, 1986.
(49) Lee, C.; Yang, W.; Parr, R. G. *Phys. Rev. B* **1988**, *37*, 785–789.
(50) Frisch, M. J.; Trucks, G. W.; Schlegel, H. B.; Scuseria, G. E.; Robb, M. A.; Cheeseman, J. R.; Montgomery, J. A.; Vreven, J., T.; Kudin, K. N.; Burant, J. C.; Millam, J. M.; Iyengar, S. S.; Tomasi, J.; Barone, V.; Mennucci, B.; Cossi, M.; Scalmani, G.; Rega, N.; Petersson, G. A.; Nakatsuji, H.; Hada, M.; Ehara, M.; Toyota, K.; Fukuda, R.; Hasegawa, J.; Ishida, M.; Nakajima, T.; Honda, Y.; Kitao, O.; Nakai, H.; Klene, M.; Li, X.; Knox, J. E.; Hratchian, H. P.; Cross, J. B.; Adamo, C.; Jaramillo, J.; Gomperts, R.; Stratmann, R. E.; Yazyev, O.; Austin, A. J.; Cammi, R.; Pomelli, C.; Ochterski, J. W.; Ayala, P. Y.; Morokuma, K.; Voth, G. A.; Salvador, P.; Dannenberg, J. J.; Zakrzewski, V. G.; Dapprich, S.; Daniels, A. D.; Strain, M. C.; Farkas, O.; Malick, D. K.; Rabuck, A. D.; Raghavachari, K.; Foresman, J. B.; Ortiz, J. V.; Cui, Q.; Baboul, A. G.; Clifford, S.; Cioslowski, J.; Stefanov, B. B.; Liu, G.; Liashenko, A.; Piskorz, P.; Komaromi, I.; Martin, R. L.; Fox, D. J.; Keith, T.; Al-Laham, M. A.; Peng, C. Y.; Nanayakkara, A.; Challacombe, M.; Gill, P. M. W.; Johnson, B.; Chen, W.; Wong, M. W.; Gonzalez, C.; Pople, J. A. *Gaussian 03*; *Rev. C.02* Gaussian, Inc.: Wallingford, CT, 2004.
(51) Dennington, R., II; Keith, T.; Millam, J.; Eppinnett, K.; Hovell, W. L.; Gilliland, R. Semichem, Inc.: Shawnee Mission, KS, 2003.

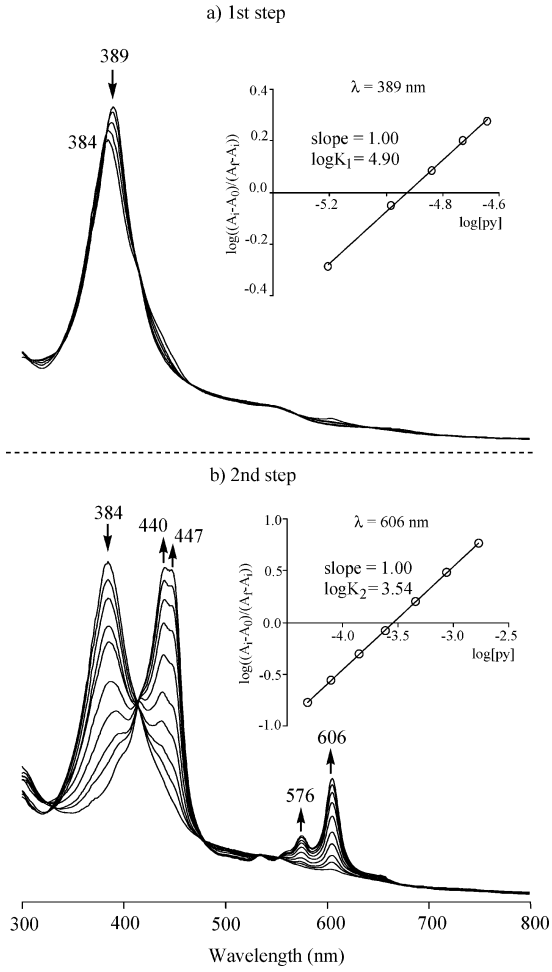

Figure 2. UV−vis spectral changes of $(F_5PhMes_2Cor)Co$ (**2**) in CH_2Cl_2 upon addition of pyridine to solution. The inset of each figure shows the Hill plot used to analyze the data. The pyridine concentration for the plots ranges from (a) 6.24×10^{-6} to 2.29×10^{-5} M and (b) 4.78×10^{-5} to 1.67×10^{-3} M.

formal Co(I) corrole, and multiple one-electron oxidations, the exact number of which will depend upon the compound substituents, type of axial ligands, and positive potential limit of the nonaqueous solvent.[4,7,21] The Co(III)/Co(II) reactions of **1**−**3** are all reversible in CH_2Cl_2, THF, or PhCN but irreversible and shifted to more-negative potentials in pyridine. The ill-defined cathodic reduction peak in py and negative shift of $E_{1/2}$ from the Co(III)/Co(II) processes in the other solutions is due to the large pyridine binding constants for the Co(III) form of the corrole and a coupled chemical reaction associated with the electron transfer.[7,22] This was verified in the present study by spectrally monitoring the binding of pyridine in a CH_2Cl_2 solution containing the cobalt corrole **2**. The spectral changes are shown in Figure 2, and the pyridine binding constants were calculated as log $K_1 = 4.90$ and log $K_2 = 3.54$ by analysis of the data.

In comparison to previously characterized cobalt corroles with four or five phenyl substituents at the β-positions of the macrocycle, such as $(Me_4Ph_5Cor)Co$,[7] the Co(III)/Co(II) redox potential of **1** and **2** in CH_2Cl_2, PhCN, or THF are shifted to more positive values due to the strong electron-withdrawing effects of the pentafluorophenyl group at the *meso*-positions of the corrole macrocycle. $(Mes_3Cor)Co$ **3**

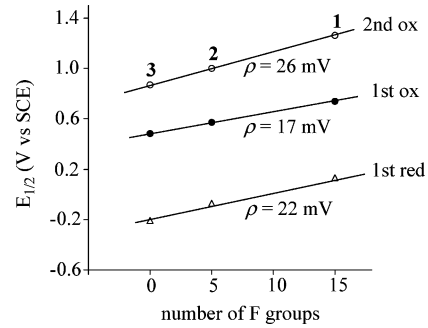

Figure 3. The relationship between the half-wave potentials and number of fluorine groups for **1**−**3** during the first and second oxidations and first reduction in PhCN.

($E_{1/2} = -0.21$ V in PCN) is more difficult to reduce than $(Me_4Ph_5Cor)Co$ ($E_{1/2} = -0.16$ V[7]), but $E_{1/2}$ values for the first oxidation of the *meso*-substituted corrole and the β-pyrrole-substituted $(Me_4Ph_5Cor)Co$ are similar to each other, being 0.48 and 0.47 V, respectively. There is also a linear trend between $E_{1/2}$ values and the number of fluorine groups on the compound for the first two oxidations and first reduction of **1**−**3** in PhCN. This is graphically shown in Figure 3 where the slope of the line amounts to 17 mV/fluorine group for the first oxidation, 26 mV/fluorine group for the second, and 22 mV/fluorine group for the first reduction. The substituent effect for the first oxidation and first reduction of the three corroles is similar to what has been reported in the case of tetraphenylporphyrins containing C_6F_5 groups at the *meso* positions of the macrocycle.[52]

As seen in Figure 1, the reduction of **2** to its formal Co(I) form is irreversible in CH_2Cl_2 and is located at $E_p = -1.58$ V for a scan rate of 0.1 V/s. This process is, however, reversible in the other three solvents and occurs at $E_{1/2} = -1.60$ to -1.68 V versus SCE for the same compound in PhCN, THF, and pyridine. The fact that the second reduction of the Co(III) corroles is not strongly affected by a change in solvent is consistent with a lack of axial ligand binding to the Co(II) and Co(I) forms of the compound.

The first reversible oxidation of **1**−**3** in CH_2Cl_2 and PhCN ranges from $E_{1/2} = 0.48$ to 0.89 V depending upon the solvent and macrocycle and this reaction is followed by up to two additional electron abstractions as seen in Figure 1 and Table 1. The second oxidation of the corroles is located at $E_{1/2} = 0.86$ to 1.18 V in CH_2Cl_2, THF, or PhCN (Table 1) but is not observed in pyridine due to the limited positive potential range of this solvent. The *meso*-substituted corroles **1**−**3** do not dimerize in CH_2Cl_2 as reported for the β-aryl-substituted corroles,[7] and this can be attributed to the presence of the bulky *meso*-aryl substituents on the macrocycle.

UV−vis Spectroelectrochemistry of $(F_5PhMes_2Cor)Co$ (2). The neutral, singly oxidized, and singly or doubly reduced corroles were spectrally characterized in the different solvents and a summary of the data for **2** is given in Table 2. Similar sets of spectral changes were obtained for the other two compounds.

(52) Kadish, K. M.; Royal, G.; Van Caemelbecke, E.; Gueletti, L. In *The Porphyrin Handbook*; Kadish, K. M., Smith, K. M., Guilard, R. Eds.; Academic Press: Boston, 2000; Vol. 9, pp 1−220.

Table 2. UV-vis Spectral Data of Neutral and Electroxidized or Electroreduced (F_5PhMes_2Cor)Co (**2**) in Different Solvents

central metal	electrode rxn	solvent	λ nm ($\varepsilon \times 10^{-4}$ M^{-1} cm^{-1})				
Co(III)	none	CH_2Cl_2	389 (5.98)		544 (0.76)		
		THF	404 (4.63)		532 (0.71)		
		PhCN	388 (5.09)				
		pyridine	442 (4.22)	450 (4.28)	537 (0.55)	577 (0.80)	607 (1.58)
Co(II)	reduction	CH_2Cl_2	421 (5.17)			569 (0.89)	
		THF	419 (4.66)			572 (0.74)	
		PhCN	426 (4.87)			574 (0.83)	
		pyridine	419 (4.60)	435[a] (2.93)		595 (0.75)	
Co(I)	reduction	CH_2Cl_2	[b]				
		THF	419 (5.71)				
		PhCN	421 (5.45)				
		pyridine	419 (5.45)			574 (0.70)	
Co(IV)	oxidation	pyridine	414 (3.86)	427 (3.82)			687 (0.32)
		PhCN	413 (5.04)	424 (4.81)			684 (0.39)
		THF	411 (3.99)	424 (3.55)			
		CH_2Cl_2	387 (3.76)	424[a] (2.29)			

[a] Shoulder. [b] Electroreduced compound reacts with solvent.

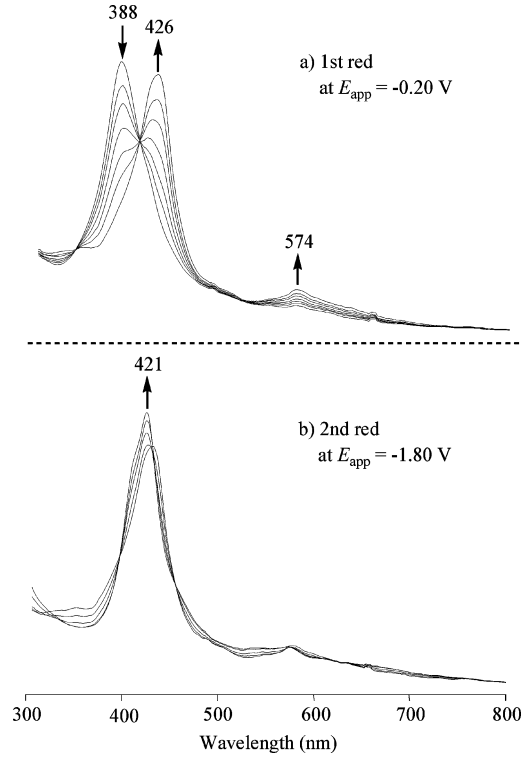

Figure 4. UV−vis spectral changes of (F_5PhMes_2Cor)Co (**2**) during the (a) first and (b) second reductions in PhCN containing 0.1 M TBAP.

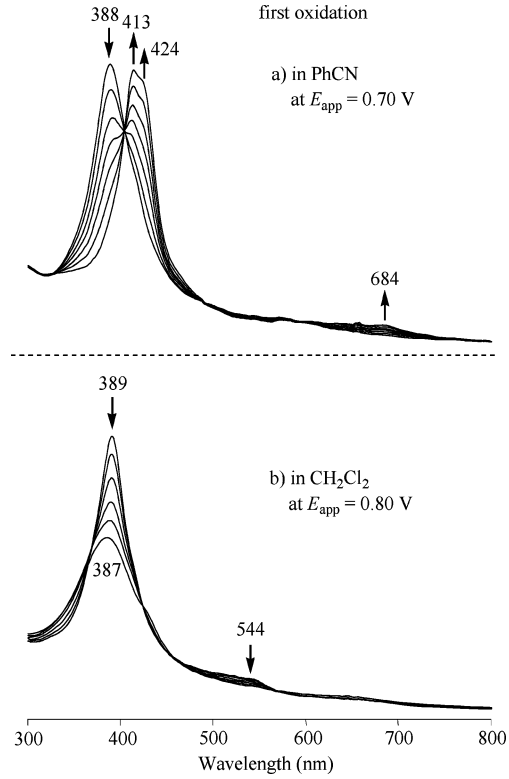

Figure 5. UV−vis spectral changes of (F_5PhMes_2Cor)Co (**2**) during the first oxidation in (a) PhCN and (b) CH_2Cl_2 containing 0.1 M TBAP.

The neutral Co(III) corrole **2** has a well-defined Soret band at 388 nm in PhCN, and this band decreases in intensity and red-shifts to 426 nm as the Co(II) form of the corrole is electrogenerated (part a of Figure 4). There are no major visible bands for the neutral corrole in PhCN, but a weak band grows in at 574 nm when the first reduction proceeds at an applied potential of −0.20 V. No radical marker bands are observed between 600∼800 nm during the first reduction, and this is consistent with the first process involving a Co(III)/Co(II) metal-centered reaction as previously described in the literature.[1,2]

The controlled reducing potential in the thin-layer cell was then switched to −1.80 V and the resulting spectral changes are shown in part b of Figure 4. As the reaction proceeded, the 426 nm band assigned to the Co(II) corrole increased in intensity and was shifted to 421 nm at the complete of the reaction. These types of spectral changes can be interpreted in terms of a metal-centered electron addition rather than a ring-centered process where a decreased intensity Soret band and broad absorption in the near-IR region of the spectrum would be expected. The assignment of a Co(II)/Co(I) process was also made in an earlier study, which reported the electrocatalytic reduction of CO_2 in CH_3CN by the doubly reduced corrole **1**.[20]

UV−vis spectral changes during the first oxidation of **2** in PhCN are shown in part a of Figure 5. The 388 nm band of the neutral Co(III) corrole red-shifts during the oxidation, giving a product with a split Soret band at 413 and 424 nm and a broad band in the near-IR at 684 nm. There are multiple well-defined isosbestic points in the spectra, indicating formation of a single oxidation product. The lack of a

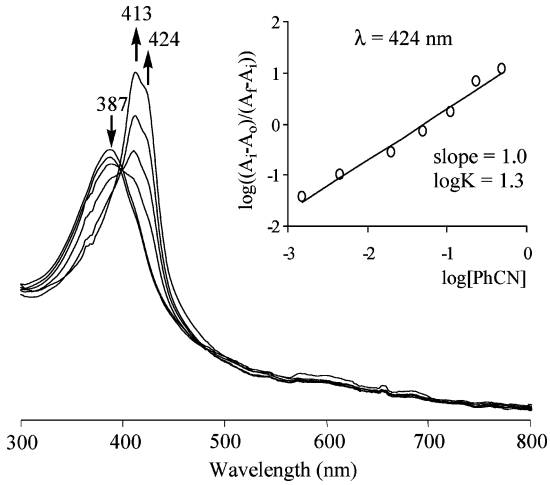

Figure 6. UV−vis spectral changes of (F_5PhMes_2Cor)Co (**2**) by addition of PhCN in CH_2Cl_2 at a controlled potential of 0.80 V.

decreased intensity Soret band for the singly oxidized corrole strongly suggests Co(IV) formation,[21] but the presence of a band at 684 nm suggests a corrole radical cation, which is also the conclusion from ESR spectra of the electroxidized species presented on the following pages.

Surprisingly, quite different spectral changes are observed during the first oxidation of **2** in CH_2Cl_2 (part b of Figure 5). In this solvent, the one-electron oxidized corrole has a decreased-intensity Soret band at 387 nm, suggesting formation of a corrole radical cation, but the expected radical marker band between 600 and 800 nm is not observed. The fact that the UV−vis spectra in both solvents have dual characteristics of a metal- and macrocycle-centered oxidation might be interpreted as a solvent-dependent change in the site of the electron transfer or it could simply be a difference in the degree of coordination, changing from four-coordinate in CH_2Cl_2 to five- or six-coordinate in PhCN. This was investigated in the present study by monitoring changes in the UV−vis spectrum of a CH_2Cl_2 solution containing singly oxidized **2** with increasing amounts of added PhCN. The results of this titration are shown in Figure 6, where the PhCN was added stepwise to $\mathbf{2}^+$ in CH_2Cl_2 while maintaining a constant controlled potential of 0.80 V to keep the oxidized species in solution. As seen in this figure, the 387 nm Soret band of the singly oxidized corrole red-shifts during the titration and leads to a species that has a split band at 413 and 424 nm. This spectrum is exactly the same as the spectrum obtained after a one-electron oxidation of **2** in neat PhCN (part a of Figure 5). A Hill plot was constructed (inset of Figure 6) and gives a straight line with a slope of 1.0, indicating that one PhCN molecule binds to the cobalt center of the singly oxidized species under the given experimental conditions. The equilibrium constant for this ligand addition reaction was calculated as $\log K = 1.3$ from the zero intercept of the plot, and the reaction can be described by eq 1.

$$[(F_5PhMes_2Cor)Co]^+ + PhCN \rightleftharpoons [(F_5PhMes_2Cor)Co(PhCN)]^+ \quad (1)$$

We earlier demonstrated that chloride ions strongly bind to the unoxidized (Me_4Ph_5Cor)Co in CH_2Cl_2[7] and similar reactions are observed for **2** as seen in part a of Figure 7 which shows the UV−vis spectral changes upon addition of TBACl to solution. The changes in absorbance of the 389 nm band were analyzed as a function of added Cl^- concentration and a plot of $\log((A_i - A_o)/(A_f - A_i))$ versus log[TBACl] gives a slope of 1.0. This means that only one chloride ion binds to the Co(III) center of the uncharged neutral compound. The intercept from the Hill plot is $\log K_1 = 2.3$ which is similar to the $\log K = 2.88$ for the chloride binding reaction of (Me_4Ph_5Cor)Co.[21] This is not surprising because **3** and (Me_4Ph_5Cor)Co have virtually the same $E_{1/2}$ values for the first oxidation, indicating a similar electron density on the metal center.

A stabilization of the higher oxidation states of **2** by the binding of Cl^- is also observed and this results in a negative shift of $E_{1/2}$ for the first two oxidations of the corrole with increasing concentration of chloride ion in solution. This is shown in part b of Figure 7 where the addition of excess Cl^- shifts both oxidation processes toward more-negative potentials. The $E_{1/2}$ for the first electron abstraction in CH_2Cl_2 shifts by 63 mV per 10-fold change in log [TBACl] (part b of Figure 7), and this indicates that the singly oxidized corrole contains one more bound chloride ion than the neutral form of the compound. Thus, the electrode reaction for the first oxidation in chloride-containing media can be described as shown in eq 2.

$$[(F_5PhMes_2Cor)CoCl]^- + Cl^- \rightleftharpoons [(F_5PhMes_2Cor)CoCl_2]^- + e \quad (2)$$

The second oxidation of **2** is also negatively shifted with increasing concentration of Cl^-, and this is shown by the cyclic voltammograms in part b of Figure 7, where the $E_{1/2}$ goes from 0.98 V in CH_2Cl_2, 0.1 M TBAP to 0.34 V after addition of 51.3 equiv of TBACl and then remains at this potential with further increases in [Cl^-].

Similar, but not identical UV−vis spectra, are obtained for the singly oxidized corrole **2** in CH_2Cl_2 and PhCN solutions containing 0.1 M TBACl. As the first oxidation proceeds at an applied potential of 0.35 V, the Soret band at 397 nm (CH_2Cl_2) or 410 nm (PhCN) decreases in intensity and shifts to 415 nm in CH_2Cl_2 and 427 in PhCN. The 553 nm band (in CH_2Cl_2) or 557 nm band (in PhCN) disappears, and a new band at 716 nm (CH_2Cl_2) or 722 nm (PhCN) appears as the electron abstraction proceeds (Figure 8). The final UV−vis spectrum in both cases is assigned to a bis-Cl^- complex, $[(F_5PhMes_2Cor)CoCl_2]^-$.

ESR Characterization of the Singly Oxidized Cobalt Corrole. The site of the electron-transfer oxidation was examined by ESR characterization of the singly oxidized cobalt corrole **2**. These spectra, obtained by the chemical oxidation of **2** with 1 equiv of $[Fe(bpy)_3]^{3+}$ (bpy = 2,2′-bipyridine) in CH_2Cl_2 and PhCN are shown in parts a and b of Figure 9, respectively. The observed g value (2.0032) is the same under both solution conditions and is characteristic of an organic radical; it is quite different from the large g

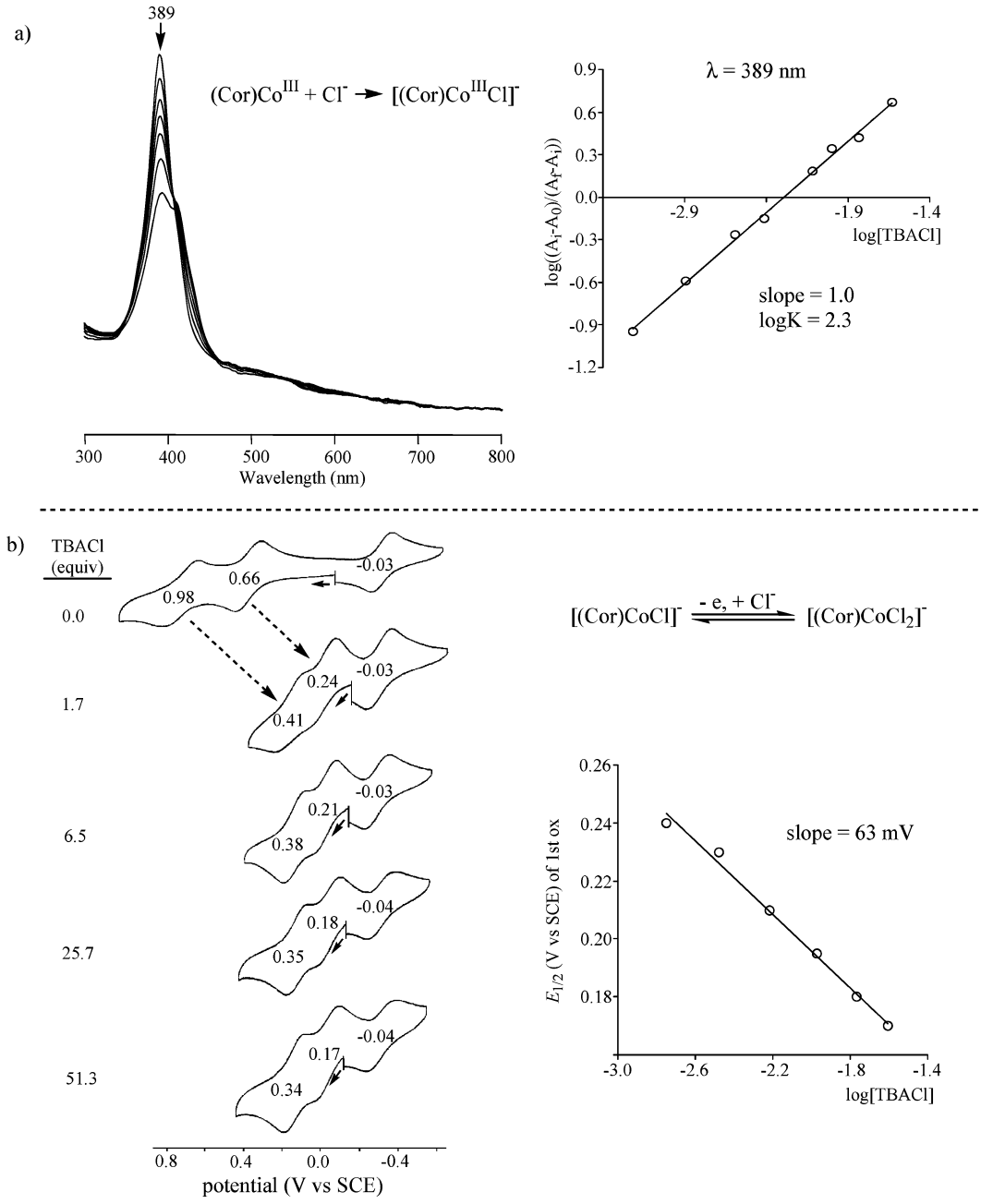

Figure 7. (a) UV−vis spectral changes for (F_5PhMes_2Cor)Co (**2**) in CH_2Cl_2 upon addition of Cl^- to solution and (b) dependence of $E_{1/2}$ on the concentration of TBACl added to solutions of CH_2Cl_2 containing 0.1 M TBAP.

value (2.037) observed for Co(IV) porphyrin complexes.[53] Thus, the singly oxidized species is assigned as a Co(III) corrole radical cation rather than as a Co(IV) corrole. The same ESR spectrum is obtained by the oxidation of **2** by O_2 in the presence of $HClO_4$ (part c of Figure 9). Similar radical cation ESR spectra were also obtained for $\mathbf{1}^+$ (g = 2.0033) and $\mathbf{3}^+$ (g = 2.0034). Figure 10 shows HOMO orbitals calculated by DFT at the B3LYP/6−31G(d) basis set. The macrocycle-centered electron-transfer oxidation of **1**−**3** is consistent with the calculated HOMO, where no metal orbital is involved in the HOMO.

Redox Properties and Catalytic Reduction of O_2 with $HClO_4$. Because the highest activity of adsorbed cobalt porphyrins and corroles toward oxygen reduction is obtained in acid media,[32–39] we examined all compounds in aqueous solutions containing 1 M $HClO_4$. Each examined complex adsorbs strongly and irreversibly on an EPPG electrode.

Figure 11 illustrates cyclic voltammograms for (F_5PhMes_2-Cor)Co (**2**) adsorbed on an EPPG electrode. In the absence of dioxygen (curves a), the corrole exhibits a single redox process centered at $E_{1/2}$ = 0.33 V (**2**). When the same solutions are saturated with air (curves b), the responses of (F_5PhMes_2Cor)Co (**2**)-coated graphite electrodes are similar to each other and are characterized by an irreversible reduction peak located at E_{pc} = 0.24−0.25 V for a scan rate

(53) Fukuzumi, S.; Miyamoto, K.; Suenobu, T.; Van Caemelbecke, E.; Kadish, K. M. *J. Am. Chem. Soc.* **1998**, *120*, 2880–2889.

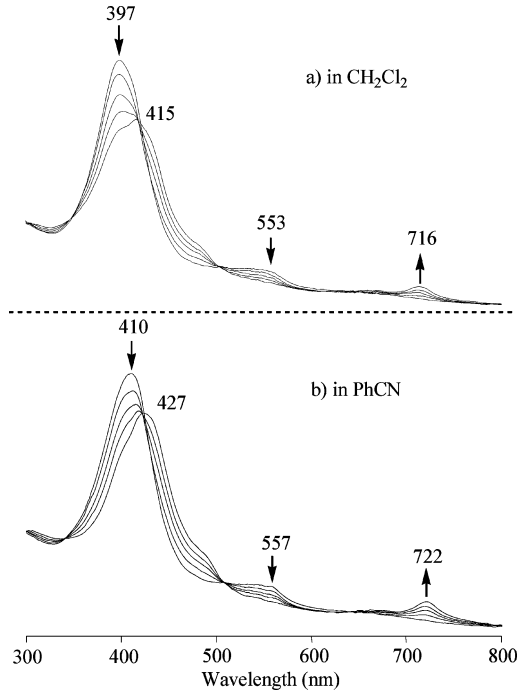

Figure 8. UV−vis spectral changes of (F_5PhMes_2Cor)Co (**2**) during the first controlled potential oxidation at 0.35 V in (a) CH_2Cl_2 and (b) PhCN containing 0.1 M TBACl.

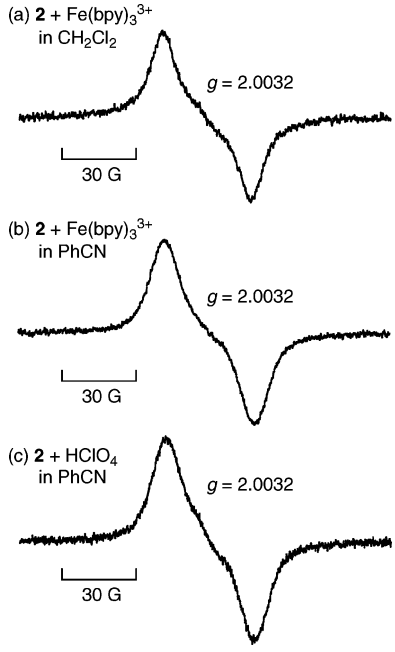

Figure 9. ESR spectra of singly oxidized **2** produced by the chemical oxidation of **2** (3.0×10^{-4} M) with (a) $Fe(bpy)_3(PF_6)_3$ (3.0×10^{-4} M) in CH_2Cl_2 at 183 K, (b) $Fe(bpy)_3(PF_6)_3$ (3.0×10^{-4} M) in PhCN at 298 K, and (c) $HClO_4$ (2.0×10^{-2} M) in aerated PhCN at 298 K.

of 50 mV/s. There is also a larger current than under an argon atmosphere as seen in Figure 11. In comparison, the reduction of O_2 at an uncoated graphite electrode occurs at a much more-negative potential ($E_p = -0.41$ V), which clearly indicates that the reactivity of the electrode upon modification with **2** must be attributed to the adsorbed cobalt corroles. The catalyzed electroreduction of O_2 by **1**, **2**, or **3** occurs at potentials similar to those for the electrode reaction of just the corrole under argon ($E_{1/2} = 0.34$ V for **1**, 0.33 V for **2**, and 0.35 V for **3**, respectively), thus indicating that the neutral Co(III) form of the cobalt corrole obtained on the electrode surface when sweeping the potential positively from +0.5 to 0.0 V catalyzes the electroreduction of O_2 in acid media as previously reported for related compounds.[31,32]

The half-wave potentials for O_2 reduction at a rotating disk electrode (Table 3) are similar for the corrole catalysts, **1**, **2**, and **3** ($E_{1/2} = 0.30$ V) and indicate that the catalytic reduction of O_2 is not strongly influenced by differences in the substitution pattern between the two compounds. However, in both cases the $E_{1/2}$ for catalytic reduction of O_2 occurs at significantly lower potential than what has been reported for previously examined cobalt monocorroles with β-pyrrole substituents, that is (Me_4Ph_5Cor)Co ($E_{1/2} = 0.38$ V);[31] the potentials are also lower than when the catalysts are (PCY)H_2Co,[21] (PCY)FeClCoCl,[32] or (PCY)MnClCoCl,[32] which show an average $E_{1/2}$ of 0.34 V for O_2 electroreduction. The shift in redox potential for the oxidation process of (TPFCor)Co (**1**), (F_5PhMes_2Cor)Co (**2**), and (Mes_3Cor)Co (**3**) may be explained by the greater bulkiness of the *meso*-substituents on the compounds. In both cases, the methyl and fluoro groups at the ortho positions of *meso*-phenyl group would prevent their rotation due to a strong repulsion by the pyrrole hydrogens.[42,54] As pointed out by Yamazaki et al.,[54] the bulkiness and orientation of these substituents should decrease $\pi-\pi$ interactions between the macrocycles and the electrode surface, and this would result in a negative shift of the half-wave potential for O_2 reduction.

To calculate the number of electrons transferred in the catalytic electroreduction of dioxygen, voltammetric measurements were also performed at a rotating disk electrode (RDE). The RDE responses of (F_5PhMes_2Cor)Co (**2**) adsorbed on the graphite electrode in 1 M $HClO_4$ (part a of Figure 12) show a single wave for the reduction of O_2. Similar behavior is observed for the tris(pentafluorophenyl) derivative **1** and trimesityl derivative **3** (data not shown). The half-wave potentials are located at 0.30 V for both compounds (at $i = 0.5i_{max}$, where i_{max} is the limiting current measured at 100 rpm), and both $E_{1/2}$ values become more negative at higher rotation rates. The number of electrons transferred during oxygen reduction was calculated from the magnitude of the steady-state limiting current values, which were taken at a fixed potential on the catalytic wave plateaus of the different current−voltage curves in part a of Figure 12 (−0.1 V). If mass transport alone controls the reduction of dioxygen at the **2**-modified electrode, then the relationship between the limiting current and rotation rate should obey the Levich equation:[55]

$$i_{Lev} = 0.62nFA\upsilon^{-1/6}D^{2/3}[O_2]\omega^{1/2} \quad (3)$$

where n is the number of electrons transferred, F is the Faraday constant (96 485 C mol^{-1}), A is the electrode area (cm^2), ν is the kinematic viscosity of the solution (cm^2 s^{-1}), D is the dioxygen diffusion constant (cm^2 s^{-1}), $[O_2]$ is the

(54) Yamazaki, S.-I.; Yamda, Y.; Ioroi, T.; Fujiwara, N.; Siroma, Z.; Yasuda, K.; Miyazaki, Y. *J. Electroanal. Chem.* **2005**, *576*, 253–259.
(55) Bard, A. J.; Faulkner, L. R. *Electrochemical Methods: Fundamentals and Applications*, 2nd ed.; John Wiley & Sons, Inc: New York, 2001.

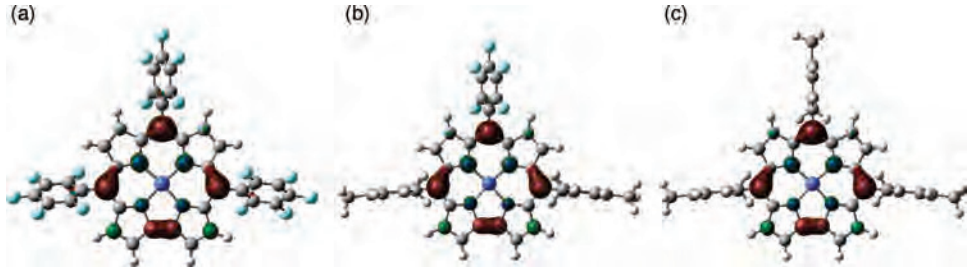

Figure 10. HOMO orbitals of (a) (TPFCor)Co (**1**), (b) (F_5PhMes_2Cor)Co (**2**), and (c) (Mes_3Cor)Co (**3**) calculated at the B3LYP/6−31G(d) level.

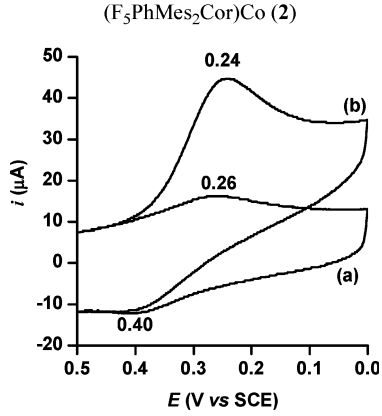

Figure 11. Cyclic voltammograms of (F_5PhMes_2Cor)Co (**2**) adsorbed on EPPG electrode. Supporting electrolyte: 1 M $HClO_4$ (a) saturated with argon and (b) saturated with air. Scan rate: 50 mV/s.

Table 3. Electroreduction of Dioxygen by Cobalt Corroles in Air-Saturated 1 M $HClO_4$

compound	E_p[a]	$E_{1/2}$[b]	n[c]
(TPFCor)Co (**1**)	0.25	0.30	2.0
(F_5PhMes_2Cor)Co (**2**)	0.24	0.30	2.0
(Mes_3Cor)Co (**3**)	0.25	0.30	2.2

[a] Peak potential of the dioxygen reduction wave (V vs SCE). [b] Half-wave potential (V vs SCE) for dioxygen reduction at rotating disk electrode (ω = 100 rpm). [c] Electrons consumed in the reduction of O_2 as estimated from the slope of the Koutecky−Levich plots.

bulk concentration of oxygen (mol dm^{-3}), and ω is the rate of rotation (rad s^{-1}).

From eq 3, the plot of the limiting current density j ($j = i/A$) as a function of the square root of the electrode rotation rate $\omega^{1/2}$ should be a straight line intersecting the origin. Part b of Figure 12 shows that the Levich plot[56] of the plateau currents versus $\omega^{1/2}$ is curved as is typical for the electroreduction of O_2 catalyzed by adsorbed cobalt complexes.[57] The clear lack of linearity in the Levich plot suggests that the catalytic reaction is limited by kinetics, not by mass transport. A chemical step, previously assigned to the formation of a cobalt(III)−O_2 adduct,[58] precedes the electron transfer and limits the current to values below the convection-diffusion limit.

The reciprocal of the limiting current density was plotted against the reciprocal of the square root of the rotation rate (Figure 12c). The straight line obeys the Koutecky−Levich equation:[59,60]

$$\frac{1}{j} = \frac{1}{nFk[O_2]} + \frac{1}{0.62nFv^{-1/6}D^{2/3}[O_2]\omega^{1/2}} \qquad (4)$$

For large values of $\omega^{1/2}$ ($\omega \rightarrow \infty$), the current is controlled by the kinetic process and reaches an asymptotic maximum value, j_k (mA cm^{-2}), which can be obtained experimentally from the intercept of the Koutecky−Levich line in part c of Figure 12,

$$jk = 10^3 nF\Gamma k[O_2] \qquad (5)$$

where k is the second-order rate constant of the reaction (M^{-1} s^{-1}), which limits the plateau current, and Γ (mol cm^{-2}) is the surface concentration of **2** and the other terms have their usual significance as described previously. The slope of the Koutecky−Levich plot shows that the catalytic electroreduction of O_2 by **2** is a two-electron process. The Koutecky−Levich plot for **1** and **3** (not shown) also indicates a two-electron reduction of O_2 to H_2O_2 (Table 3) as previously reported in the literature.[35] In contrast, the number of electrons transferred is 2.9 for (Me_4Ph_5Cor)Co,[31] indicating that the catalytic electroreduction of O_2 by the cobalt complex leads to the formation of H_2O and H_2O_2 through processes involving both two-electron and four-electron reactions. The catalytic activity of this β-pyrrole-substituted corrole was attributed to the spontaneous dimerization (and higher aggregation) of the complex on the electrode surface.[31] Such a van der Waals-driven association has also been reported for unsubstituted cobalt porphyrins[46,61] and is believed to create cobalt−cobalt separations that are small enough to permit O_2 molecules to coordinate simultaneously to two cobalt centers. One result of such an orientation at the electrode surface is a weakening of the O−O bond, which would favor its breaking during the four-electron reduction of O_2 to H_2O.[46,62] In the case of **1**−**3**, the two-electron reduction of O_2 clearly indicates that a dimerization (or oligomerization) does not occur for either complex, and this is consistent with the expected steric interactions involving the bulky phenyl *meso*-substituents.[61]

The j_k value obtained from the intercept of part c of Figure 12 was used to calculate the second-order rate constant k for the formation of the (F_5PhMes_2Cor)$Co^{III}O_2$ complex on the electrode surface. The value calculated at pH 0 using eq 5 is $k = 1.7 \times 10^5$ M^{-1} s^{-1}, which is lower than that for the catalytic electroreduction of dioxygen at the (Me_4Ph_5Cor)Co

(56) Levich, V. G. *Physicochemical Hydrodynamics*; Prentice-Hall, Inc.: Englewood Cliffs, N. J., 1962.
(57) Liu, H.-Y.; Abdalmuhdi, I.; Chang, C. K.; Anson, F. C. *J. Phys. Chem.* **1985**, *89*, 665–670.
(58) Chang, C. J.; Loh, Z.-H.; Shi, C.; Anson, F. C.; Nocera, D. G. *J. Am. Chem. Soc.* **2004**, *126*, 10013–10020.
(59) Koutecky, J.; Levich, V. G. *Zh. Fiz. Khim.* **1958**, *32*, 1565–1575.
(60) Oyama, N.; Anson, F. C. *Anal. Chem.* **1980**, *52*, 1192–1198.
(61) Song, E.; Shi, C.; Anson, F. C. *Langmuir* **1998**, *14*, 4315–4321.
(62) Shi, C.; Steiger, B.; Yuasa, M.; Anson, F. C. *Inorg. Chem.* **1997**, *36*, 4294–4295.

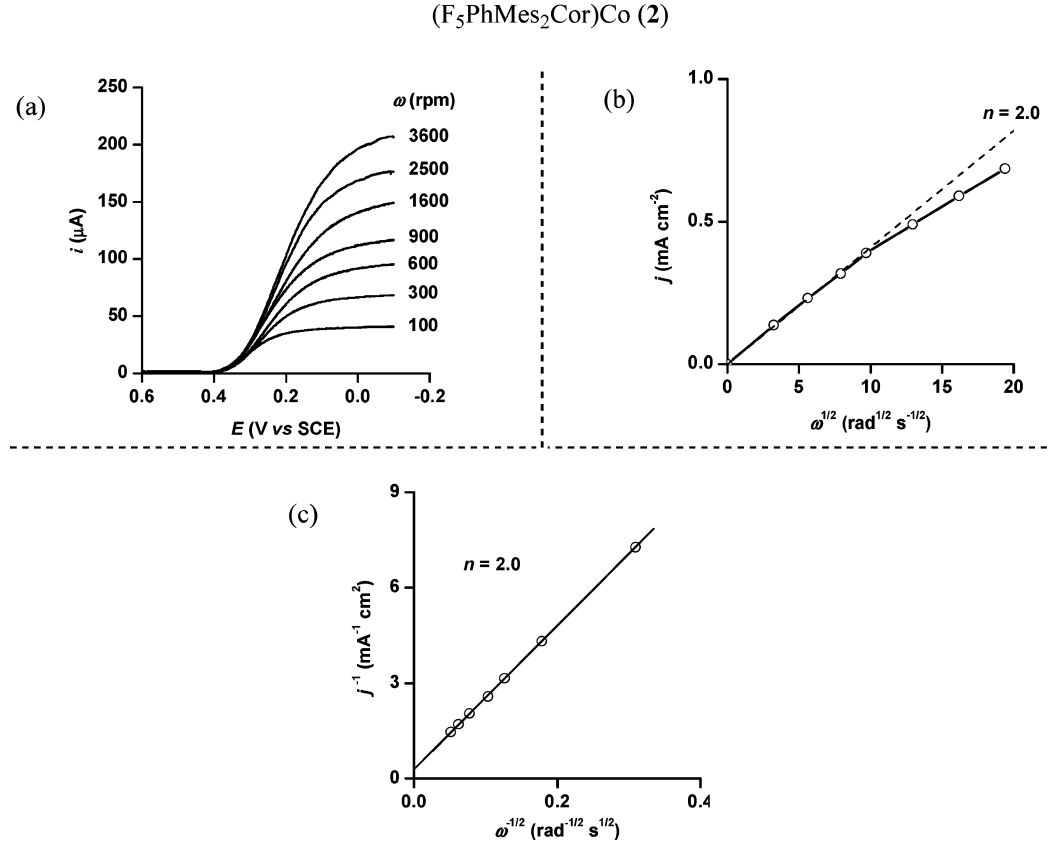

Figure 12. Catalyzed reduction of O_2 in 1 M $HClO_4$ at a rotating graphite disk electrode coated with (F_5PhMes_2Cor)Co (**2**). (a) Values of the rotation rates of the electrode (ω) are indicated on each curve. The disk potential was scanned at 5 mV s^{-1}. (b) Levich plots of the plateau currents of (a) vs (rotation rate)$^{1/2}$. The dashed line refers to the theoretical curve expected for the diffusion-convection limited reduction of O_2 by $2e^-$. (c) Koutecky−Levich plots of the reciprocal plateau currents vs (rotation rates)$^{-1/2}$. Supporting electrolyte: 1 M $HClO_4$ saturated with air.

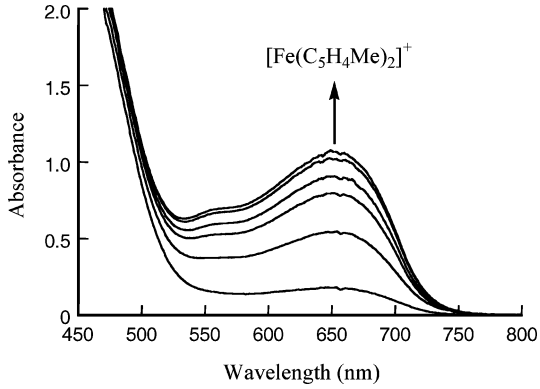

Figure 13. Visible absorption spectral changes in the catalytic reduction of O_2 (1.7×10^{-3} M) by $Fe(C_5H_4Me)_2$ (2.0×10^{-2} M) in the presence of $HClO_4$ (2.0×10^{-2} M) and **2** (2.0×10^{-5} M) in PhCN at 298 K.

modified electrode ($k = 5.7 \times 10^5$ M^{-1} s^{-1}) but is identical to a value reported for the electrocatalytic reduction of O_2 by the cobalt porphyrin (diethylesterMe$_2$Et$_2$P)Co ($k = 1.4 \times 10^5$ M^{-1} s^{-1}).[36]

Catalytic Reduction of O_2 in the Homogeneous Phase. The catalytic two-electron reduction of O_2 with cobalt corroles was confirmed for the homogeneous phase using 1,1′-dimethylferrocene $Fe(C_5H_4Me)_2$ as a reductant in PhCN. No oxidation of $Fe(C_5H_4Me)_2$ by O_2 occurred in the presence of $HClO_4$ in PhCN at 298 K but the addition of (F_5PhMes_2Cor)Co (**2**) to an air-saturated MeCN solution of $Fe(C_5H_4Me)_2$ and $HClO_4$ resulted in efficient oxidation of ferrocene by O_2. Figure 13 shows formation of the 1,1′-dimethylferricenium ion $[Fe(C_5H_4Me)_2]^+$ during reduction of O_2 (1.7×10^{-3} M) by a large excess of $Fe(C_5H_4Me)_2$ (2.0×10^{-2} M) in the presence of a catalytic amount of **2** (2.0×10^{-5} M) and $HClO_4$ (2.0×10^{-2} M). The concentration of $[Fe(C_5H_4Me)_2]^+$ (3.4×10^{-3} M) formed in the catalytic reduction of O_2 by $Fe(C_5H_4Me)_2$ is twice that of the O_2 concentration (1.7×10^{-3} M). Thus, only a two-electron reduction of O_2 occurs, and there is no further reduction to produce more than 2 equiv of $[Fe(C_5H_4Me)_2]^+$ (eq 6).

$$2Fe(C_5H_4Me)_2 + O_2 + 2H^+ \xrightarrow[(F_5PhMes_2Cor)Co\ \ (2)]{} 2[Fe(C_5H_4Me)_2)]^+ + H_2O_2 \quad (6)$$

In a similar manner, **1** and **3** also catalyze the two-electron reduction of O_2 by $Fe(C_5H_4Me)_2$ in the presence of $HClO_4$ and give as a corrole oxidation product the Co(III) π-cation radical, $[(^{\cdot}Cor)Co^{III}]^+$, as indicated in an earlier section of the manuscript.

Summary and Conclusions

In summary, we have shown that cobalt corroles can be used as effective catalysts in the reduction of O_2 with $HClO_4$ via the redox couple between Co(III) corroles and

Co(III) corrole radical cations. The site of electron-transfer oxidation is clearly identified as macrocycle centered by detection of the ESR signal for the Co(III) corrole radical cation. Koutecky−Levich plots for the *meso*-substituted corroles **1**−**3** indicate a two-electron reduction of O_2 to H_2O_2. The catalytic activity of the previously studied β-pyrrole-substituted complex $(Me_4Ph_5Cor)Co$ involves both two-electron and four-electron transfer reactions, and this is attributed to spontaneous dimerization (and higher aggregation) of the complex on the electrode surface. Dimerization does not occur for the *meso*-substituted corroles, and here only the two-electron transfer pathway is observed.

Acknowledgment. The support of the Robert A. Welch Foundation (K.M.K., grant E-680), the French Ministry of Research (MENRT), CNRS (UMR 5260) and the Ministry of Education, Culture, Sports, Science and Technology, Japan (grant 19205019 and a Global COE program, the Global Education and Research Center for Bio-Environmental Chemistry) are gratefully acknowledged. We also acknowledge the assistance of Wiroaj Kajonkijya for collection of the O_2 electrocatalytic reduction data using **3** as a catalyst.

IC800458S